

Numerical Studies of Directional Wavemaker Performance

John F. O'Dea¹ and J. Nicholas Newman²
(¹Carderock Division, Naval Surface Warfare Center,
²MIT (Emeritus) and WAMIT, Inc.)

ABSTRACT

The performance of a multi-unit wavemaker for generating directionally-spread waves has been studied using the three-dimensional, radiation-diffraction code WAMIT. Design choices of wavemaker geometry (including type of motion, total number of units and size of individual units) affects various parameters of performance, including quality of radiated waves and inertial loads that actuators must overcome. The sensitivity of generated waves to these variables is demonstrated.

INTRODUCTION

Wavemakers have been in use in ship testing tanks for about a century. The earliest were typically driven by a constant rpm motor through reduction gears and a bell crank or eccentric to produce oscillatory motion of a bulkhead or plunger. These wavemakers were typically installed at the end of long, narrow tanks so that testing in long-crested head and following waves was possible. As understanding of the random nature of ocean waves improved, and servo-type control systems became available, more realistic generation of random waves with specified statistical properties became possible.

At the Naval Surface Warfare Center, Carderock Division (NSWCCD), wavemakers are installed in both the long narrow basins of David Taylor Model Basin (DTMB) and in the wide Maneuvering and Seakeeping Basin (MASK). The MASK Basin is rectangular, 110 m long by 70 m wide. It has wavemakers on two adjacent sides, with beaches on opposite sides. The beaches take up 10 m of each dimension, so that the wavemakers are 100 and 60 m wide, respectively (referred to the Long Bank and the Short Bank). The basin is 6 m deep, except for an 11 m deep trench adjacent to the beach along the 110 m side.

When the Maneuvering and Seakeeping (MASK) Basin at Carderock was being designed in the 1950's, pneumatic-type wavemakers were chosen. Pneumatic wavemakers were installed in the other basins as prototypes of increasing size before the MASK was built, culminating in a full-size prototype in the Deep basin of DTMB. A 1:10 scale model of the complete MASK geometry was also constructed and tested, (Marks 1958). These wavemakers consist of air-filled domes at the water surface, with the air pressure changed in an oscillatory manor by a system of blowers and diverter valves. Pneumatic wavemakers were chosen on the basis of their mechanical simplicity (Brownell 1956). However, they have several drawbacks. Pressurized air is introduced at discrete locations in the domes, giving rise to transverse variation of pressure and water sloshing that is difficult to suppress. Furthermore, the transfer function of this type of wavemaker (amplitude of generated wave per unit control input, as a function of frequency) is complicated, with several peaks and nodes, and nonlinear behavior is difficult to control or compensate. Finally, the wavemaker installation in the MASK consists of a relatively small number of wide units (8 on the Short Bank and 13 on the Long Bank), making the generation of waves at an oblique angle to the wavemakers impractical. Instead, the MASK was designed with a moveable bridge from which the towing carriage is suspended. This bridge can be rotated up to 45 deg, allowing towed models to be tested in oblique, long-crested waves. By using both banks simultaneously it has been possible to test in waves with two directional components (such as seas and cross-swell), but only for the case where the two components are individually long-crested, and are at exactly 90 degrees relative to each other.

The demands of modern ship designs have provided a strong incentive to replace the MASK wavemakers with a modern system capable of

generating waves with a wide range of characteristics, including short-crested random waves with specified spectral density and directional spreading function. The approach described here is a numerical one, based on three-dimensional linearized potential flow. All computations are done in the frequency domain. The emphasis is on understanding the characteristics of the wave field for nominally unidirectional (long-crested) regular waves, with the expectation that a properly designed control system can superimpose components to generate irregular short-crested waves of specified characteristics. It is recognized that the generation of steep waves will require further analysis of nonlinear effects, but it was felt that this linear approach is a necessary first step in determining overall wavemaker characteristics such as width and depth of individual units, maximum stroke and power requirements, and total number of wavemaker units.

TYPES OF WAVEMAKERS

Wavemakers installed in test tanks today are typically either hinged flaps (rotating about a pivot point below the still water level), or translating pistons as shown in Figure 1.

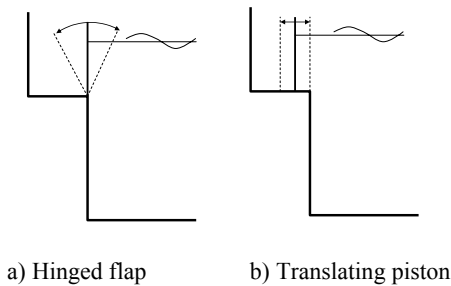


Figure 1: Geometry of wavemakers.

Hinged flaps are more commonly found in deep-water tanks (water depth large compared to typical wave lengths), while pistons are more commonly found in shallow tanks used to study coastal waves, Tsunamis, etc. The reason for these choices is not difficult to see: since the motion of the wavemaker face is primarily horizontal, the motion should ideally approximate the variation of the horizontal wave orbital motion with depth below the free surface. In deep water ($\lambda < h$), this variation will tend to be exponential with depth, while in very shallow water ($\lambda \gg h$) there is little decay of the horizontal orbit from the surface to the bottom. For hinged flaps in deep tanks, the linear variation of horizontal motion with depth is chosen as a compromise to approximate the

desired motion over the design range of wavelengths. Some flap-type wavemakers have been built with dual, articulated flaps to better approximate the exponential variation with depth, although at the additional complication and expense of twice the number of actuator mechanisms and controls. Piston wavemakers have also been built with horizontal articulation to better approximate the phase variation when generating oblique waves, described by Burcharth et al (1986), although this requires a more complicated joint and seal mechanism.

Note that no type of wavemaker can exactly match the desired orbital motion of the generated waves. This results in a local (evanescent) disturbance that does not propagate into the far field but will be present in the near field in front of the wavemaker. The local pressure on the face of the wavemaker also results in a force (or moment) that must be considered in the actuator design for the wavemaker. This effect is typically represented as a frequency-dependent added mass and damping, similar to what is used in typical ship motion calculations. The inability to exactly match a sinusoidal phase variation, when generating oblique waves, is another practical limitation on all wavemaker systems.

TWO-DIMENSIONAL WAVEMAKER THEORY

The linear, potential flow theory for generation of waves by oscillating solid boundaries was first solved by Havelock (1929), who derived the analytical solution for both two- and three-dimensional wavemakers. This was applied by Biesel and Suquet (1954) to the geometry of a hinged flap (hinge axis at the bottom of a basin), and by Hyun (1976) to cases where the wavemaker does not extend to the full depth of the basin. The linear transfer function $H(\omega) = A/S$ between the wave amplitude (A) and wavemaker stroke (S) has been experimentally confirmed in many basins (Ursell et al (1960), Hudspeth et al (1981)), and has also been extended to nonlinear wave generation both by an expansion to 2nd order (Sulisz and Hudspeth (1993), Schaffer (1996), Lee et al (1998)) and in fully nonlinear calculations (the “numerical wave tank”). It will be shown below that a three-dimensional wavemaker, when operating with all units in phase, has transfer functions for added mass and radiated waves similar to the two-dimensional case but with local fluctuations.

THREE-DIMENSIONAL WAVEMAKERS

If a wide wavemaker is subdivided into a sufficiently large number of narrow boards, and these individual boards are controlled in such a way that the phase of motion varies along the width of the wavemaker, waves are generated at an oblique angle to the face of the wavemaker. Such wavemakers, often called snake- or serpentine-type wavemakers, have been installed in a number of wide basins (Biesel and Suquet (1954), Madsen (1974), Nohara (2000)). To generate waves at an angle β to the x-axis, with time dependence $e^{i\omega t}$, the spatial phase relationship is:

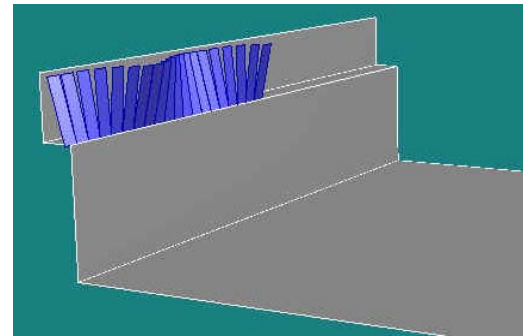
$$e^{-ik(x \cos \beta + y \sin \beta)} \quad (1)$$

When generating oblique waves from two adjacent, perpendicular wavemaker banks, the amplitude of the wavemaker stroke also has to be adjusted by $\sin\beta$ and $\cos\beta$ on the wavemakers along the X and Y axes respectively, to maintain the same amplitude of propagating wave. As pointed out by Ogilvie (1963), secondary waves at other headings are also generated because of the finite width of the wavemaker (an open boundary is assumed at one end, representing perfect absorbing beaches in the MASK), and the finite width of individual wavemaker boards when they are phased as above. The control system driving the individual wavemaker boards should account for these effects in order to provide maximum uniformity of the waves over the maximum possible extent of a basin.

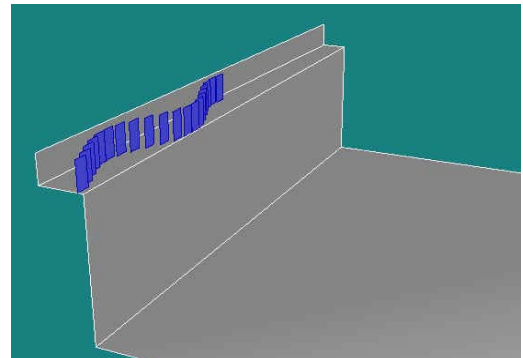
Three wavemaker geometries will be examined, where the phase is varied along the wavemaker bank to produce oblique waves:

- a) hinged paddles rotating about a horizontal axis
- b) translating pistons
- c) horizontally-articulated pistons, in which relative rotation between boards is about a vertical axis at the connection between boards, and the actuators drive the connection point.

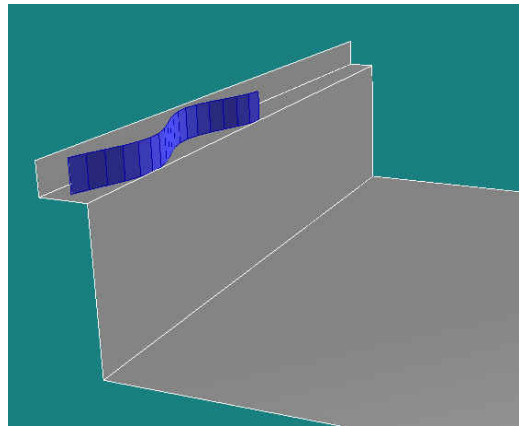
These geometries are illustrated in Figure 2.



a) Hinged flap



b) Translating piston



c) Horizontally-articulated piston

Figure 2: Geometry of phased, three dimensional wavemakers.

NUMERICAL APPROACH

The capability to analyze 3D wavemakers is included in the radiation/diffraction code WAMIT (see Section 10.8 of WAMIT, Inc.). For the special case where the wavemakers are located in one or two planes of symmetry, the solution is given explicitly by appropriate distributions of sources of known strength, proportional to the normal velocity of the wavemakers, and it is not necessary to solve the usual integral

equation for the velocity potential unless there are other bodies within the wave tank. This configuration corresponds to a tank with rectangular walls in the planes of symmetry. The opposite walls are assumed to have absorbing beaches, represented by open domains extending to infinity.

Since the solution is explicit, the computational burden is greatly reduced. On the other hand, when a description of the radiated wave field is required over a large array of field points, it is important to use efficient algorithms especially for the evaluation of the free-surface Green function or wave source. The approach used for the present results is based on the higher-order option where each wavemaker element is represented by a single ‘patch’ with specified geometry, and the source distribution is continuous on each patch. The surface integrations are performed with Gaussian quadratures. The normal velocity on each wavemaker is defined in a DLL subroutine, and can be designated in whatever way is most appropriate.

For the present computations each wavemaker is a rectangular element, and the vertical variation of the normal velocity with depth is either constant (piston) or linear about a specified hinge depth (flap). Different distributions of the velocity along the bank are considered including piecewise constant (where each element is independent) and ‘tent functions’ for the horizontally-articulated piston (where the velocity is continuous between adjacent elements).

SAMPLE RESULTS

a) Single Narrow Unit

A single, narrow unit is the fundamental “building block” of a three-dimensional directional wavemaker. For waves of length greater than the unit width, the wave field produced by this single unit is expected to be qualitatively that of a pulsating free-surface source.

As shown in Figure 3a), the waves from a single unit radiate outward in a circular pattern of decreasing amplitude, with a wavelength equal to the plane wave of the same period (about 6 m in this example). When the waves are generated in the presence of a reflecting wall (on the x-axis), the effect is the same as having an image source (located at $y = -30$ m in this example), and the combined waves from the two sources create an interference pattern.

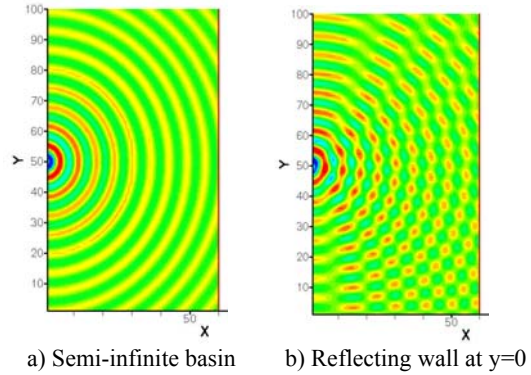


Figure 3: Wave field generated by single unit, period = 2 sec, wavemaker unit centered at $y = 30$ m, 1 m wide.

b) Long (But Finite Extent) Wavemaker Along One Wall, All Boards in Phase

The wavemaker is a hinged paddle, hinge depth = 2 m below the free surface. The wavemaker extends from $y = 0$ to $y = 100$ m, with an adjacent wall along the x-axis (reflecting wall) and the domain extending to infinity in the positive x- and y-directions (no beach reflection). With all boards in phase, the wavemaker generates quasi-two dimensional waves, as shown in Figure 4 which is a snapshot at time $T=0$. However, variations in crest amplitude are seen, both along each crest and at the free end of the wavemaker ($y > 100$ m)

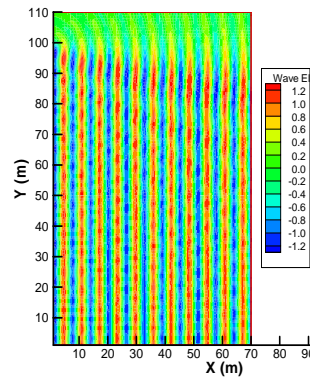


Figure 4: Waves generated by wavemaker along the y-axis, $0 < Y < 100$ m, period = 2 sec, reflecting wall at $y = 0$.

Figure 5 shows the amplitude of the wave, along a line parallel to the nominal wave crest, for periods of 1.4 and 2.0 sec. The variation is most noticeable toward the free end of the wavemaker, but can be seen throughout the range of y from 0 to 100 m.

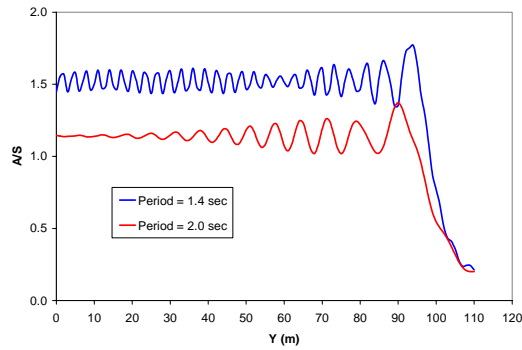


Figure 5: Variation of wave amplitude along a line at $x = 20$ m from the wavemaker, all units in phase.

A similar variation is seen in the force on the face of the wavemaker, Figure 6. This force can be resolved into an added mass and damping coefficient as shown. The damping is associated with the energy being put into the wave that progresses into the far field. The added mass is associated with the pressure in the evanescent wave system that does not propagate. Both of these force components must be considered in designing actuators for a wavemaker system. In addition to the added mass and damping, the mechanical inertia of the wavemaker board itself must be included,

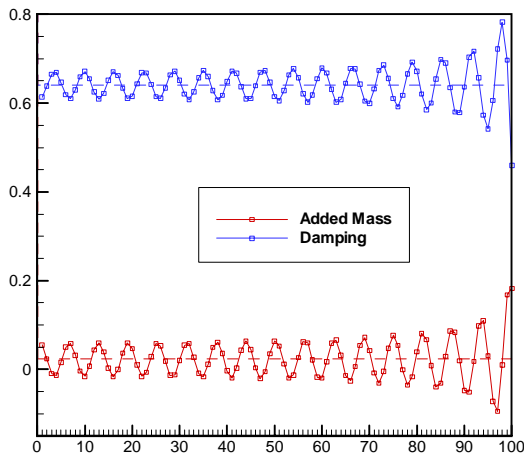


Figure 6: Variation of added mass (lower curve) and damping coefficient (upper curve) along 100 m wavemaker, all units in phase, period = 2 sec. Horizontal axis is board index, starting near the x-axis (reflecting wall).

Although there is spatial variation in the 3D results, at a point in the center of the MASK domain

there is still close correlation to the purely 2D results for a narrow basin, as shown in Figure 7,

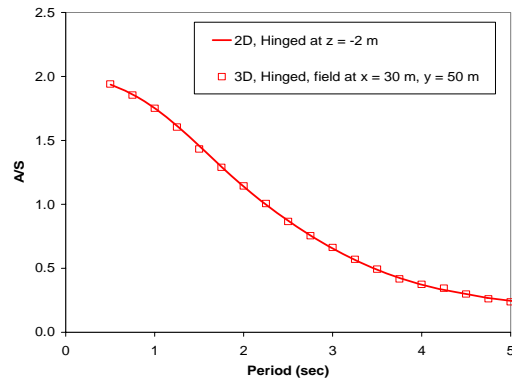


Figure 7: Comparison of 2D and 3D wavemaker transfer functions.

The variation of the wave amplitude indicates that it should be possible to at least partly compensate for this variation, by adjusting the amplitude and phase of the actuator signals when there is a sufficient number of individual boards, especially near the free end of the wavemaker. An example is shown in Figure 8. In this case, the gain was smoothly tapered to zero along the last 10% of the length toward the free end ($90 < Y < 100$). No phase adjustment was attempted. It can be seen that this simple “smoothing” of the otherwise abrupt discontinuity of board motion, at the free end of the wavemaker, noticeably reduces the variability of the wave amplitude. More sophisticated methods of determining the wavemaker drive signal, including both amplitude and phase adjustments, should result in further improvements to the uniformity of the wave field in the basin, as shown by Matsumoto and Hanzawa (1996).

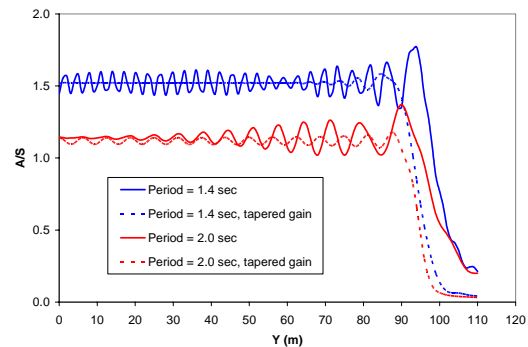


Figure 8: Effect of tapering wavemaker gain in reducing spatial fluctuation of generated waves, $x = 20$ m, 0 deg wave direction.

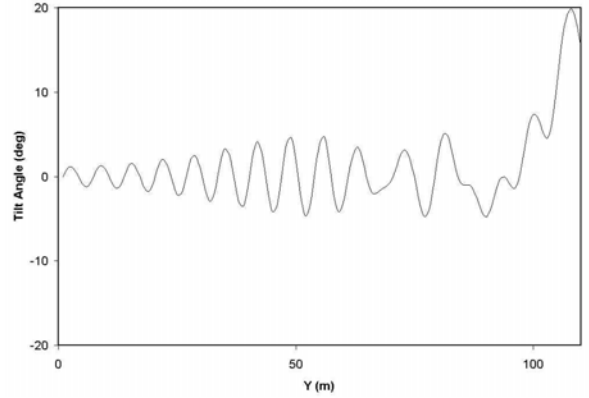
Another measure of deviation of the wave field from a long-crested, two dimensional wave can be found by studying the horizontal velocities in the wave field. WAMIT includes an option to calculate the velocity components,

$$\begin{aligned} V_x &= |V_x| \cos(\omega t + \alpha_x), \\ V_y &= |V_y| \cos(\omega t + \alpha_y) \end{aligned} \quad (2)$$

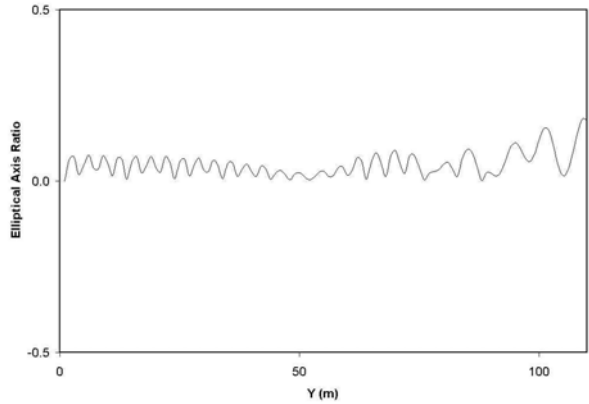
These are the components of an elliptical motion in the horizontal plane. The parametric form of an ellipse can be written as:

$$\begin{aligned} \xi &= a \cos \theta, \\ \eta &= b \sin \theta \end{aligned} \quad (3)$$

Thus, if the major and minor axes a, b are aligned with the global coordinate system in which the hydrodynamic computations are done, then V_x, V_y will have a phase difference of exactly 90 degrees. This is generally not the case in the three-dimensional computations presented here. However, the components calculated in the global (x, y) coordinates can be used to calculate the major and minor axes of the elliptical motion, the angle of tilt of the major axis relative to the nominal wave direction, and the eccentricity (ratio of minor to major axis). These quantities provide insight into the deviation of the flow field from that of an ideal, long-crested progressive wave. An example is shown in Figure 9.



a) Angle of major axis



b) Eccentricity

Figure 9: Angle of major axis, and eccentricity of elliptical motion in horizontal plane for 100 m wide wavemaker, period = 2 sec, nominal wave direction = 0 deg.

c) Wavemaker Along One Wall, Oblique Waves Generated by Phasing Board Motions

When the motions of the individual; wavemaker units are phased according to equation (1), a beam of oblique waves is generated, together with the secondary waves seen in the previous case. A snapshot at time = 0 is shown in Figure 10. Examples of the wave amplitude 30 m from the wavemaker, and forces on the wavemaker boards, are shown in Figures 11 and 12.

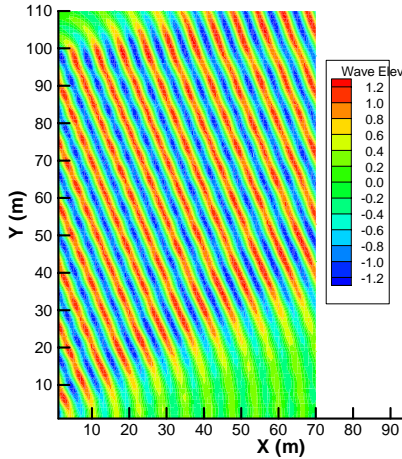


Figure 10: Wave elevation contours, oblique wave generation, period = 2 sec, direction = 22.5 deg.

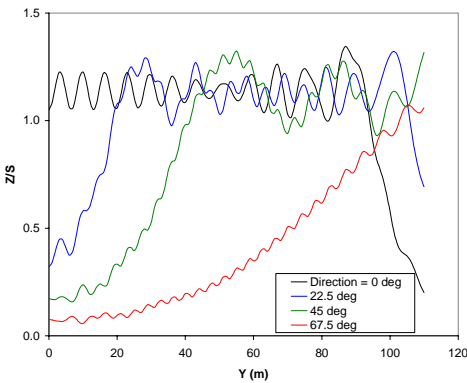


Figure 11: Wave amplitude variation, oblique wave generation, period = 2 sec, x = 30 m.

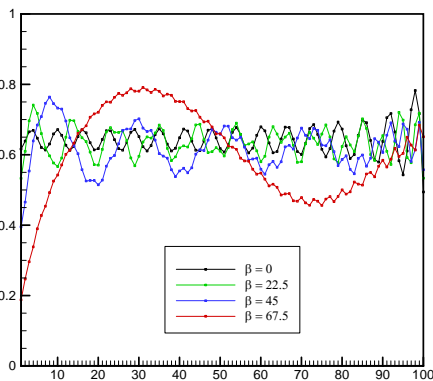


Figure 12: Force amplitude on each board of 100m wavemaker, for normal ($\beta=0$) and oblique wave generation, period = 2 sec. The amplitude of each element at the free surface is $\cos(\beta)$. Horizontal axis is board index, starting at $y = 0$ (reflecting wall).

d) Sensitivity studies for oblique wave generation.

The sensitivity of wave generation to various wavemaker design parameters has been examined. A larger number of narrower wavemaker boards will obviously allow the snake-type phasing in oblique waves to more closely follow a smooth, continuous function. A comparison of 50, 100, and 150 boards is shown in Figures 12-14. The total wavemaker length is kept at 100 m, so that the individual boards are 2 m, 1 m and 2/3 m, respectively. Figure 12 shows the wave amplitude variation for a wave direction of 45 deg and 2 sec period. The wave magnitude is shown at $x = 30$ m away from the wavemaker (mid-basin). The results for 100 and 150 boards are virtually identical, while there is only a small reduction for the 50 wider boards. Figure 13 shows a more demanding case: the wave period is shorter (1.4 seconds), with a fundamental wavelength of about 3 m, and the wave length of the snake-type phased notion is slightly more than 4 m, or twice the width of the coarsest board geometry. In this case the results for the 2 m board width show a strong secondary wave. Finally, Figure 15 shows the results for an even more demanding situation, with a nominal wave direction of 67.5 deg (close to parallel to the wavemaker along the y-axis) and period of 1.4 sec. In this case the wavelength of the phased motion is less than two board widths for the 2 m boards, and the results are badly aliased.

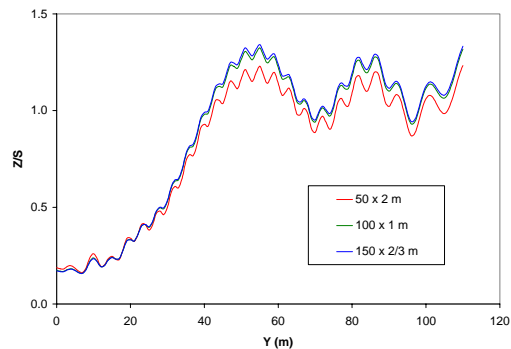


Figure 13: Wave amplitude for 50, 100 and 150 boards, 45 deg direction, 2 sec period, x = 30 m, hinged paddles.

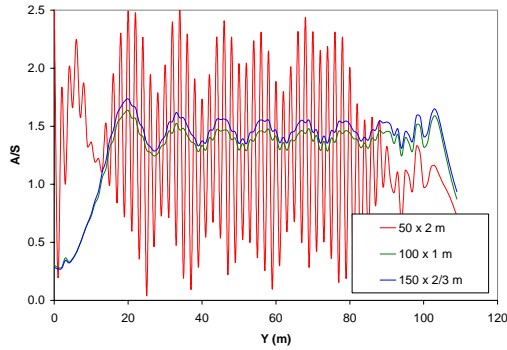


Figure 14: Wave amplitude for 50, 100 and 150 boards, 45 deg direction, 1.4 sec period, $x = 10$ m.

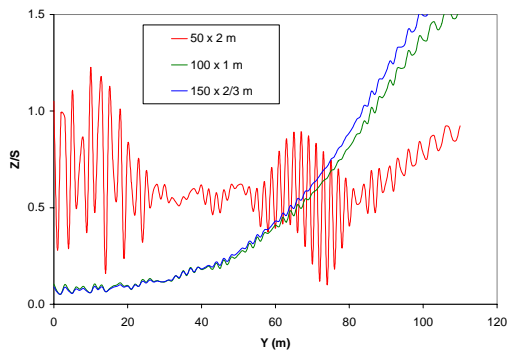


Figure 15: Wave amplitude for 50, 100 and 150 boards, 67.5 deg direction, 1.4 sec period.

Other options studied include a piston-type wavemaker, operating both as a series of parallel pistons with discontinuous displacement in oblique wave generation (see Figure 2b) and with horizontal articulation so that the displacement is piecewise-linear in oblique wave generation (see Figure 2c). It was found that, to achieve a similar transfer function (A/S) to that of the hinged paddle type wavemaker over the normal wave period range in the MASK, a piston wavemaker would have to extend into the basin less than half the depth of the hinged paddle, as shown in Figure 16.

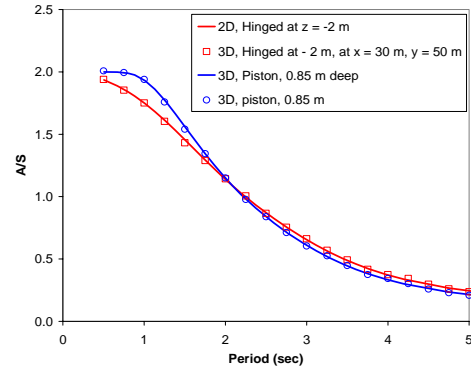


Figure 16: Comparison of hinged paddle and piston wavemaker transfer function (A/S).

The use of a piston-type wavemaker also makes it possible to use a horizontal articulation (see Figure 2c) in which the actuators force a translational motion at the joint between wave boards. The result is a continuous, piecewise-linear (rather than discontinuous), variation of the wavemaker displacement when oblique waves are generated. This has the potential of reducing the irregularities in the waves caused by the discontinuities seen in Figures 2a and 2b). Figure 17 shows the wave amplitude fluctuation at a distance of 30 m from the wavemaker bank, comparing the discontinuous piston and the horizontally-articulated (tent) piston mode. The 100 m long wavemaker is resolved into a coarse (33 boards), medium (50) and fine (100) spatial discretization. There does not appear to be any obvious advantage to the “tent” mode in this example, and in fact the overall magnitude of the wave in the middle of the basin ($x = 30$ m) is somewhat reduced when the tent mode is employed. The large-scale fluctuations are believed to be a consequence of the finite width of the total wavemaker, rather than the finite width of the individual boards.

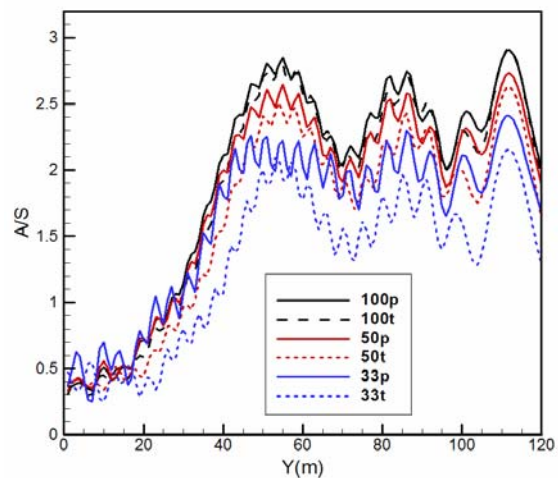


Figure 17: Effect of horizontal articulation on uniformity of generated oblique waves, 2 second period, 45 degree direction, $x = 30$ m. Wavemaker divided into 100 x 1 m, 50 x 2 m, and 33 x 3 m boards. p = piston, t = tent (horizontally articulated piston).

e) Complete oblique wave system, wavemakers operating along two adjacent walls.

The final example simulates the operation of a complete directional wavemaker, with wave boards operating on two adjacent, perpendicular walls. The example is for a 2 second wave period, with wave boards phased to produce a nominal wave direction of 67.5 degrees relative to the x-axis. Figure 18 shows a snapshot in time of the wave field, first as generated by a bank of 60 x 1 m wide boards along the x-axis, then by a bank of 100 x 1 m boards along the y-axis, and finally with both banks operating together.

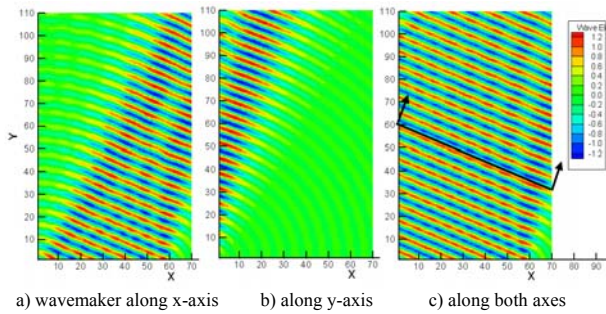


Figure 18. Oblique wave field generated by wavemakers a) along x-axis, b) along y-axis, and c) both operating together. Wave period = 2.0 sec, nominal wave direction = 67.5 deg relative to x-axis.

Illustrations such as Figure 18 help to provide an overall qualitative impression of the behavior of the wave field. More detailed quantitative information can be provided by plotting various quantities of interest, such as the wave amplitude along a cut through the wave field (such as the heavy black line in Figure 18c), see Figure 19, or the hydrodynamic force acting on the wavemaker boards, Figure 20.

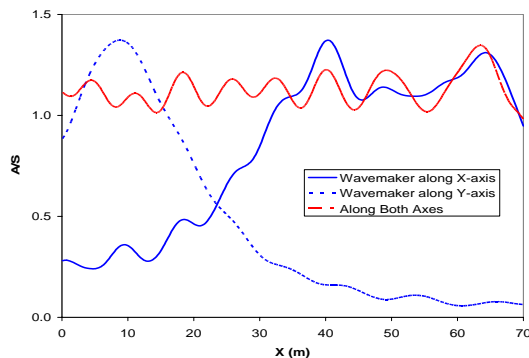


Figure 19: Variation in wave amplitude along a line parallel to nominal crest direction, centered at $x = 30$ m, $y = 45$ m (heavy line in Figure 18c).

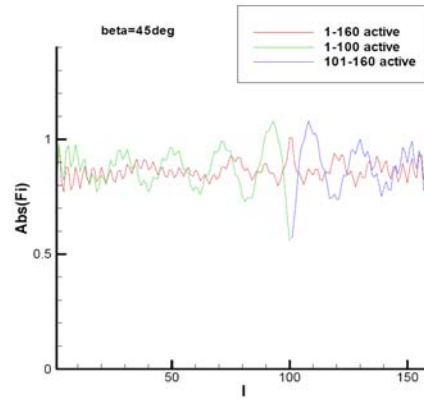


Fig 20: Hydrodynamic force on wave boards in oblique wave generation.

A quantitative impression of variability of the wave field is obtained by plotting the wave amplitude, plus the properties of the elliptical horizontal motion, along several lines parallel to the nominal crest direction as shown in Figure 21.

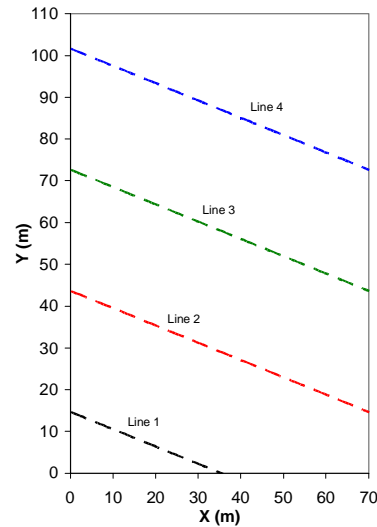


Figure 21: Lines parallel to nominal crest line, for mapping variation of wave characteristics

The variability of wave amplitude is shown in Figure 22. With the exception of the ends of the lines with $x > 60$ m (beyond the end of the wavemaker on the x-axis), the variability in amplitude is generally within $\pm 5\%$. The variability in wave direction, as shown in the horizontal orbital motion in Figure 23, is generally within ± 5 degrees, except near $x = 0$ and $x > 60$ m, and the eccentricity of the elliptical horizontal motion is less than 0.10, as shown in Figure, with the exceptions noted above.

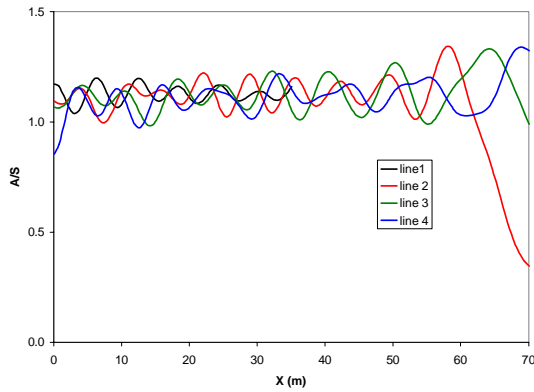


Figure 22: Variation of wave amplitude in obliquely generated waves.

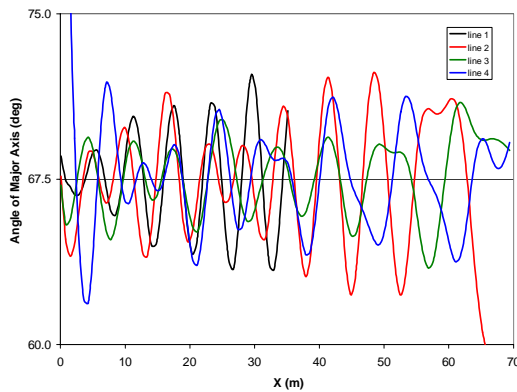


Figure 23: Variation of direction angle in obliquely generated waves.

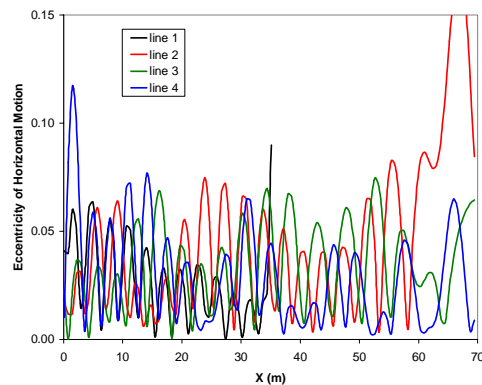


Figure 24: Variation of horizontal orbit eccentricity in obliquely generated waves.

DISCUSSION AND CONCLUSIONS

The results presented here clearly show that, while phasing of a bank of narrow wavemaker units can produce waves that are at an oblique direction relative to the wavemaker, careful tuning of the signals sent to each wavemaker unit will be required in order to minimize variability of the wave amplitude and direction. Tradeoffs will be required in the design of a wavemaker, balancing an acceptable level of variability against the cost of building and maintaining a large number of wavemaker boards. One possible criterion for acceptable variability would be to reduce the spatial variations below the level of statistical variability expected in any practical model test in random waves.

Once the variability is reduced to an acceptable tolerance, it should be possible to generate a random wave with specified frequency spectrum and directional characteristics, within the limits of small wave steepness and linear potential flow theory. Further studies will be required to determine the importance of nonlinear and viscous effects. These effects will be important in the generation of steep waves and when the phase shift along a bank of wavemaker boards is abrupt enough to cause significant discontinuities at the joints between adjacent boards.

Further studies using the numerical approach described here can be extended to simulation of random, directionally spread waves. One challenge in testing in such a wave field is the actual measurement of the directional spectrum. Directional waves are typically measured either by several methods. One method uses an array of discrete elevation measurements (or bottom-mounted pressure measurements when water depth is small). Another method measures the motion of a floating buoy, including vertical acceleration and pitch/roll (tilt) motions with suitable calibration of the buoy's response characteristics. Yet another uses 3D acoustic Doppler velocity measurements to estimate the directional orbital spectrum, which in turn leads to the directional wave elevation spectrum. All of the wave field properties used in these measurement devices can be simulated using the numerical approach described here.

ACKNOWLEDGEMENTS

This work was funded by internal funds of the Hydromechanics Department at NSWCCD, in support of the Facilities Division engineering effort for a new MASK wavemaker. The computational code for

calculating the horizontal elliptical orbits was provided by Dr. Michael Hughes of the Seakeeping Division, NSWCCD.

REFERENCES

Biesel, F. and F. Suquet., *Laboratory Wave-Generating Apparatus*, translation from La Houille Blanche by St. Anthony Falls Hydraulic Laboratory, Report 39, March 1954.

Brownell, W. F., *A Rotating Arm and Maneuvering Basin*, 11th American Towing Tank Conference, Bethesda, MD, September 1956.

Burcharth, H.F., Nielsen, S.R.K. and Shaarup-Jensen, K., *A Three Dimensional Sea Facility for Deep and Shallow Water Waves*, 5th OMAE Conference, Tokyo, 1986, pp. 72-79.

Havelock, T. H. *Forced Surface-Waves on Water*, Philosophical Magazine, vol. iii, October 1929, pp. 569-576.

Hudspeth, Robert T., Leonard, John W., and Chen, Min-Chu, *Design Curves for Hinged Wavemakers: Experiments*, Proceedings of ASCE, Hydraulics Division, Vol. 107, No. HY5, May, 1981, pp. 553-574.

Hyun, Jae Min, *Theory For Hinged Wavemakers of Finite Draft in Water of Constant Depth*, J. Hydronautics, Vol. 10, no. 1, Jan 1976, pp. 2-7.

Lee, Jaw-Fang, Liu, Cheng-Chi, and Lan, Yuan-Jyh, *A Second-Order Solution of the Flap Wavemaker Problem*, Proceedings of OTRC Symposium on Ocean Wave Kinematics, Dynamics and Loads on Structures, 1998, pp. 9-16.

Madsen, O. S., *A Three Dimensional Wavemaker, Its Theory and Application*, Journal Of Hydraulic Research, 1974, pp. 205-22.

Marks, Wilbur, *Wave Propagation in the tenth-Scale Model of the Maneuvering Basin Part I _ Long-Crested Regular Waves*, DTMB Report 1192, October 1958.

Matsumoto, Akira and Minoru Hanzawa, *New Optimization Method for Paddle Motion of Multi-Directional Wavemaker*, International Conference on Coastal Engineering, 1996, pp. 479-492.

Nohara, Ben T., *A Survey of the Generation of Ocean Waves in a Test Basin*, J. Brazilian Society of Mechanical Sciences, Vol. 22, No. 2, 2000.

Ogilvie, T. Francis, *Production of Oblique Waves by a Bank of Wavemakers*, Journal of Ship Research, June 1963, pp.7-13.

Schaeffer, Hemming A., *Second-Order Wavemaker Theory for Irregular Waves*, Ocean Engineering, Vol. 23, No. 1, 1996, pp. 47-88.

Sulisz, W., and Hudspeth, R. T., *Complete Second-Order Solution for Water Waves Generated in Wave Flumes*, Journal of Fluids and Structures, Vol. 7, 1993, pp. 253-268

Ursell, F., Dean, R.G., and Yu, Y.S., *Forced small-amplitude water waves: a comparison of theory and experiment*, Journal of Fluid Mechanics, Vol. 7, 1960, pp. 33-52.

WAMIT, Inc., *User Manual*, www.wamit.com.